FISEVIER

Contents lists available at ScienceDirect

# Journal of Power Sources

journal homepage: www.elsevier.com/locate/jpowsour



# Prussian blue nanocubes as cathode materials for aqueous Na-Zn hybrid batteries

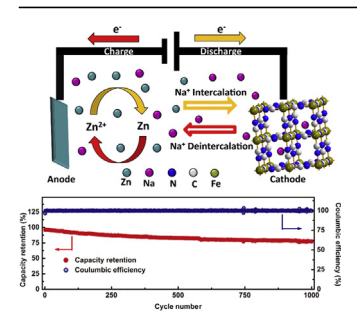


Li-Ping Wang <sup>a, b</sup>, Peng-Fei Wang <sup>a, b</sup>, Tai-Shan Wang <sup>a, b</sup>, Ya-Xia Yin <sup>a, b</sup>, Yu-Guo Guo <sup>a, b, \*\*</sup>, Chun-Ru Wang <sup>a, b, \*</sup>

#### HIGHLIGHTS

- Using Prussian blue nanocubes as cathode materials in a hybrid aqueous batteries.
- 80% capacity retention after 1000 cycles has been achieved.
- The reversible phase transition mechanism of Prussian blue is revealed.

#### G R A P H I C A L A B S T R A C T



# ARTICLEINFO

Article history: Received 22 February 2017 Received in revised form 6 April 2017 Accepted 12 April 2017

Keywords: Hybrid aqueous batteries Prussian blue Single iron-source Cycling stability Rate capability

# ABSTRACT

Rechargeable aqueous battery is very attractive as a promising alternative energy storage system, based on its safety and environmental-friendly properties. An aqueous rechargeable Na-Zn hybrid battery is assembled by using Prussian blue nanocubes and metallic zinc as cathode and anode, respectively. This Na-Zn cell delivers a high specific capacity of 73.5 mA h g $^{-1}$  and a good cycling stability (ca. 80% capacity retention after 1000 cycles at 300 mA g $^{-1}$ ) due to the impressive structure stability of Prussian blue nanocubes. These remarkable features are realized by a simple synthetic method and a feasible battery manufacturing process, which can provide guidance for the development of rechargeable batteries in a large scale.

© 2017 Published by Elsevier B.V.

*E-mail addresses*: ygguo@iccas.ac.cn (Y.-G. Guo), crwang@iccas.ac.cn (C.-R. Wang).

### 1. Introduction

In recent years, well-developed battery technology have been proposed as a possible strategy for energy storage. Especially, lithium ions batteries (LIBs) are widespread available in the portable electronics market because of their high specific capacity, long cycle life and high average voltage [1,2]. In despite of the great success of LIBs, their expensive cost and potential safety hazards

<sup>&</sup>lt;sup>a</sup> CAS Key Laboratory of Molecular Nanostructure and Nanotechnology, and Beijing National Laboratory for Molecular Sciences, Institute of Chemistry, Chinese Academy of Sciences (CAS), Beijing 100190, PR China

<sup>&</sup>lt;sup>b</sup> School of Chemistry and Chemical Engineering, University of Chinese Academy of Sciences, Beijing 100049, PR China

<sup>\*</sup> Corresponding author. CAS Key Laboratory of Molecular Nanostructure and Nanotechnology, and Beijing National Laboratory for Molecular Sciences, Institute of Chemistry, Chinese Academy of Sciences (CAS), Beijing 100190, PR China.

<sup>\*\*</sup> Corresponding author. CAS Key Laboratory of Molecular Nanostructure and Nanotechnology, and Beijing National Laboratory for Molecular Sciences, Institute of Chemistry, Chinese Academy of Sciences (CAS), Beijing 100190, PR China.

related to flammable and highly toxic organic electrolyte restrict the practical application, specifically on a large scale. In this regard, people begin to shift their attention to some aqueous-battery systems with reversible insertion of Li $^+$  [3–7], Na $^+$  [8–11], Mg $^{2+}$  [12], Zn $^{2+}$  [13–15] or hybrid [16–21] ions. These aqueous batteries use aqueous solutions, inexpensive resources, simple cell assembly technology under loose environment and do not have safety concerns [22], all of these advantages can provide this kind of battery wide applications aspect in large-scale energy storage areas.

Prussian blue (PB)  $(M_aFe[Fe(CN)_6]_b.\Box_{1-b}.mH_2O; M$ , alkaline metal;  $\square$ , [Fe(CN)<sub>6</sub>] vacancies occupied by coordinating water; 0 < a < 2, b < 1) is considered as a kind of promising cathode material. On one hand, the opening framework with the  $(C \equiv N)^-$  anions is large enough to ensure fast ionic diffusion [23–25], on the other hand, the synthetic procedure of materials are simple and adoptable [25–29]. In previous reports, Prussian blue homologue such as nickehexacyanoferrate [29] and copper hexacyanoferrate [24] were found to own good electrochemical activities in aqueous solutions. The opening structure in nickehexacyanoferrate contributes to the low voltage hysteresis between the charge/discharge processes and can insert/extract both Na<sup>+</sup> and K<sup>+</sup> in many reversible cycles [30]. Copper hexacyanoferrate can work with a high rate and shows a good cycling performance. But it is also established that the intrinsic crystal structure of PB greatly influence its electrochemical performance [31]. [Fe(CN)<sub>6</sub>] vacancies may induce lattice distortion and even hinter electron and Na<sup>+</sup> transfer, further resulting in electrochemical performance deterioration [27]. However, there have been few reports concerned Prussian blue nanocubes cathodes with low [Fe(CN)<sub>6</sub>] defects in aqueous batte-

Herein, we firstly report an aqueous Na-Zn hybrid battery system using Prussian blue nanocubes as cathode materials. This Prussian blue Na $_{0.61}$ Fe $_{1.94}$ (CN) $_{6}$ ·  $\square_{0.06}$  (NaFe-PB) cathode combine with zinc anode as a full battery, which can provide an average potential of 1.1 V and show an impressive cycling stability with 80% capacity retention even after 1000 cycles at a current density of 300 mA g $^{-1}$ .

# 2. Experimental

 $\rm Na_4Fe(CN)_6\cdot 10H_2O$  (99%) was obtained from Sigma-Aldrich, HCl (37%) was purchased from Sinopharm chemical reagent, Beijing, China. Zn foil (99.9%, 0.15 mm) was purchase from Alfa Aesar. The electrolyte was prepared by dissolving 1.0 mol  $\rm L^{-1}$   $\rm Na_2SO_4$  in deionized water.

To prepare the cathode NaFe-PB, a single iron-source method was chose. Traditionally, the PB bulk synthesis always used an aqueous solution dissolved with  $K_4Fe(CN)_6$  and metal salt [32]. During the dissolution, the relative concentrations of the precursors, the nucleation condition and reaction rate change, leading to the defects and vacancies in the final production. In order to acquire a more perfect crystal, we only used  $Na_4Fe(CN)_6 \cdot 10H_2O$  as the iron source to prepare the NaFe-PB nanocrystal to achieve a slower growing process (details in supplementary).

### 3. Results and discussion

## 3.1. Structure and morphology of NaFe-PB

Fig. 1a shows a schematic representation of hybrid  $Zn|1 \text{ mol } L^{-1} \text{ Na}_2SO_4|\text{NaFe-PB}$  battery. During the charging/discharging process, Na<sup>+</sup> inserts or extracts from the open framework channels of NaFe-PB along with the dissolution/deposition of  $Zn^{2+}$  at Zn anode in 1 mol  $L^{-1} \text{ Na}_2SO_4$  solution. The left side of Fig. 1b shows the cubic  $[Fe_2(CN)_6]^-$  framework, in which low-spin Fe<sup>II</sup> contact the carbon

atoms while high-spin Fe<sup>III</sup> contact the nitrogen atoms. Na<sup>+</sup> occupy the voids within the framework, among them, one of the energetically preferred Na<sup>+</sup> position the 24d site is shown on the right of Fig. 1b [33]. The crystalline structure of the final product was analyzed by XRD, the diffraction lines of NaFe-PB can be indexed to a pure face-centered cubic phase perfectly (Fig. 1c). Apart from that. Raman spectra (Fig. 1d) was tested to identify the valence state of Fe. Peaks of v (CN) is corresponding to the frequency of the cyanide stretching vibration mode [34]. CN<sup>-</sup> coordinated to Fe<sup>III</sup> exhibits higher wavenumber peaks than that coordinated to Fe<sup>II</sup> [25]. Therefore, two peaks of  $\nu$  (CN) at 2148 cm<sup>-1</sup>, 2090 cm<sup>-1</sup> are corresponding to CN<sup>-</sup> coordinated to Fe(III) and Fe(II), respectively. Besides, XPS measurements were also carried out for NaFe-PB. The Fe 2p peaks are presented in Fig. S1. The Fe 2p signals include Fe 2p3/2 and Fe 2p1/2. Fe 2p3/2 signal is the sum of two pairs peaks, corresponding to Fe<sup>3+</sup> and Fe<sup>2+</sup>, which is consistent with the Raman results.

The morphology of as-prepared NaFe-PB sample was characterized by SEM. The NaFe-PB samples are nanocubes with high crystallinity and these cubes have a diameter ranging from 200 nm to 700 nm (Fig. 2a and b). Moreover, no matter in high or low magnification, it is obviously to find that most crystals are intact and regular. TEM image and the EDS mappings in Fig. 2c-f clearly show that sodium, nitrogen and iron are uniformly distributed in these nanocubes. The corresponding selected area electron diffraction (SAED) pattern indicates that NaFe-PB has a strong cubic crystallographic texture. By a common method with two iron sources including Na<sub>4</sub>Fe(CN)<sub>6</sub>·10H<sub>2</sub>O and Fe(NO<sub>3</sub>)<sub>3</sub>·9H<sub>2</sub>O, the low quality Prussian blue (LO-PB) sample was produced for comparison (details in supplementary). The LQ-PB are amorphous according to the SAED (Fig. S2). The slower growing process for NaFe-PB nanocubes contributes to acquire a more perfect structure, which is further confirmed by the elemental content results obtained using EA and ICP-AES. Table S1 lists the weight percentage of N, C, H, Na and Fe for the NaFe-PB, the as synthesized product can be described by a formula  $Na_{0.61}Fe_{1.94}(CN)_6 \cdot \square_{0.06}$  and the water content of the NaFe-PB sample is around 15.7% according to the TG analysis (Fig. S3†). While the LQ-PB contains more water at 24.0% by TG, which can also prove that the NaFe-PB has lower defects.

# 3.2. Electrochemical performance of NaFe-PB-Zn hybrid aqueous batteries

The performance of NaFe-PB as cathode for aqueous batteries was evaluated by using a three-electrode glass cell. The typical CV curves (Fig. 3a) at a scanning rate of 1 mV s<sup>-1</sup> in 1 mol L<sup>-1</sup> Na<sub>2</sub>SO<sub>4</sub> solution demonstrate the characteristic potentials of the redox processes in this aqueous system. To evaluate the electrochemical stability window of the electrolyte, CV was conducted within a voltage range from -0.5-2.6 V vs  $Zn^{2+}/Zn$  electrode (-0.76 V vs NHE) at the same scanning rate of 1 mV s $^{-1}$ . Due to decomposition of water in the aqueous electrolyte, there are two significant irreversible processes evolved. One cathodic peak at -0.5 V and one anodic peak at 2.5 V can be assigned to hydrogen and oxygen evolution respectively, indicating the electrochemical stability window of the electrolyte. The two sets of reversible processes observed at 0 V attribute to the reversible deposition/dissolution of zinc. NaFe-PB shows two pair of redox peaks and these redox peaks can be attributed to the reversible conversion between Fe<sup>3+</sup> and Fe<sup>2+</sup> accompanied by the intercalation/deintercalation of Na<sup>+</sup> in different special sites of the PB framework and these processes happen within the stability window of electrolyte. Based on these results, the galvanostatic discharge and charge voltage profiles of NaFe-PB was operated in the suitable voltage range 0.9–1.6 V under a current density of 100 mA  $g^{-1}$  (Fig. 3b). From the second cycle, the

# Download English Version:

# https://daneshyari.com/en/article/5149113

Download Persian Version:

https://daneshyari.com/article/5149113

<u>Daneshyari.com</u>